

# On branches of the KS black hole

Alex Buchel

*Department of Applied Mathematics*

*Department of Physics and Astronomy*

*University of Western Ontario*

*London, Ontario N6A 5B7, Canada*

*Perimeter Institute for Theoretical Physics*

*Waterloo, Ontario N2J 2W9, Canada*

## Abstract

The Klebanov-Strassler black hole is a holographic dual to  $\mathcal{N} = 1$  supersymmetric  $SU(N) \times SU(N + M)$  cascading gauge theory plasma with spontaneously broken chiral symmetry. The chiral symmetry breaking sector of the cascading gauge theory contains two dimension-3 operators and a single dimension-7 operator. The black hole solution constructed in [1] represents the end point of the instability triggered by the condensation of one of the dimension-3 operators. We study here all three branches of the quasinormal modes of the chiral symmetry breaking sector — there are no additional instabilities beyond the one identified in [2]. Thus, the Klebanov-Strassler black hole solution of [1] is the only one with homogeneous and isotropic horizon, perturbatively connected to the chirally symmetric Klebanov-Tseytlin black hole [3].

May 2, 2020

# Contents

<b>1</b>	<b>Introduction and summary</b>	<b>2</b>
<b>2</b>	<b>Effective action, equations of motion and the boundary asymptotes for <math>\chi</math>SB QNMs of the KT black hole</b>	<b>7</b>
2.1	The effective actions . . . . .	9
2.2	KT black hole and $\chi$ SB quasinormal modes . . . . .	11
2.3	High-temperature (near-conformal) limit . . . . .	15
<b>3</b>	<b>KS branches from explicit <math>\chi</math>SB fluctuations of the KT black hole</b>	<b>18</b>
<b>A</b>	<b><math>\mathcal{B}_7</math> branch of the QNMs of the KT black hole in the <math>b \rightarrow 0</math> conformal limit</b>	<b>21</b>
<b>B</b>	<b><math>\mathcal{B}_{3u}</math> and <math>\mathcal{B}_{3s}</math> branches of the KT black hole QNMs in the <math>\sqrt{b} \rightarrow 0</math> conformal limit</b>	<b>23</b>

## 1 Introduction and summary

The Klebanov-Strassler (KS) black hole [1] is a holographic dual to a cascading gauge theory<sup>1</sup> [5] plasma in the deconfined homogeneous and isotropic state with spontaneously broken chiral symmetry. It is a “branch” of the Klebanov-Tseytlin (KT) black hole [3, 6–9] — a holographic dual to a deconfined thermal equilibrium state of the cascading gauge theory with unbroken chiral symmetry — in that it is associated with the perturbative spontaneous chiral symmetry breaking ( $\chi$ SB). In other word, there is a critical temperature [2]

$$T_{\chi\text{SB}} = 0.54195 \Lambda, \quad (1.1)$$

with  $\Lambda$  being the strong coupling scale of the cascading gauge theory [3, 10], below which the  $\chi$ SB fluctuations become perturbatively unstable. The endpoint of condensation of these fluctuations is the KS black hole [1]. The constructed KS black hole has some unusual features, when interpreted as a holographic dual of a thermal equilibrium state of the renormalizable<sup>2</sup> four-dimensional gauge theory:

---

<sup>1</sup>See [4] for the details of the holographic correspondence.

<sup>2</sup>Holographic renormalization of the cascading gauge theory was established in [9].

- (i) To begin, the KS black hole is actually neither thermodynamically nor dynamically stable — it has a negative specific heat, and correspondingly [11] an imaginary speed of the sound waves. The latter implies that the small inhomogeneities in the energy density and the pressure in the chiral symmetry broken phase of the cascading plasma amplify, destroying the homogeneity and isotropy of the corresponding thermal state.
- (ii) The phase transitions in the cascading gauge theory plasma look very different in canonical and microcanonical ensembles. From the canonical ensemble perspective, the KS black hole is an *exotic* object<sup>3</sup> — it exists only for  $T \geq T_{\chi\text{SB}}$  and has a higher free energy density as compared to that of the KT black at the corresponding temperature. It is thus irrelevant in the canonical ensemble. On the other hand, in the microcanonical ensemble, it is a dominant (more entropic) configuration below some critical energy density  $\mathcal{E}_{\chi\text{SB}}$  (associated with  $T_{\chi\text{SB}}$ ) — in a constraint (to spatial homogeneity and isotropy) dynamical evolution it is the end-point of the relaxation associated with the  $\chi\text{SB}$ .
- (iii) The  $\chi\text{SB}$  instability occurs at a lower temperatures/lower energy densities than the confinement/deconfinement phase transition in the cascading gauge theory [3],

$$T_c = 0.6141111 \Lambda > T_{\chi\text{SB}}. \quad (1.2)$$

Here the (canonical ensemble) transition proceeds from the deconfined chirally symmetric phase to a confined phase with spontaneous  $\chi\text{SB}$ . Still,  $T_{\chi\text{SB}}$  is above the temperature of the thermodynamic/dynamic instability in the KT black hole plasma [13],

$$T_{\chi\text{SB}} > T_u = 0.537286 \Lambda. \quad (1.3)$$

While unusual, (i)-(iii) can be incorporated into a consistent physics story.

- (i) and (ii) suggests that the end point of the  $\chi\text{SB}$  in the cascading plasma can simply be an inhomogeneous state; it would proceed in two steps: spontaneous symmetry breaking as in [2], followed by the relaxation to a spatially inhomogeneous equilibrium state (so far unknown). There are plenty examples of such phenomena (albeit in the presence of the chemical potential/charge density), see [14] for examples in the Nambu-Jona-Lasino-type models, and [15] for a holographic model.

---

<sup>3</sup>First examples of such objects in holography were reported in [12].

■ (iii) suggests that the confinement and the chiral symmetry breaking can be two separate transitions, see [16] for an example in a phenomenological QCD model and [17] for a holographic example. Despite (1.2), the cascading gauge theory  $\chi$ SB phase transition can still be important as it is the second-order (thus being a perturbative one) phase transition, while the confinement transition of [3] is of the first-order, proceeding through the bubble nucleation, which is strongly suppressed for a large number of colors.

Alternatively, it is possible that there are other KS black holes, beyond the construction of [1], with the more standard thermodynamics and the pattern of the phase transitions. This is the question we would like to address in this paper. It is conceivable that there exist KS black holes separated from the KT black hole by the first-order phase-transition — we can not add anything new here. Instead, we focus on potentially additional “branches” of the KS black holes, connected to the KT black hole “trunk” via instabilities in the chiral symmetry breaking sector. The reason why one might expect additional branches is related to the richness of the chiral symmetry breaking sector: as explain in [2], this sector involves linearized gravitational fluctuations dual to a pair of dimension-3 operators and a single dimension-7 operator. Thus, from the holographic bulk perspective one expects three distinct branches of the quasinormal modes (QNMs) of the KT black hole. Only a single branch (referred to as  $\mathcal{B}_{3u}$  here) was identified in [2].

In what follows, we identify all the three branch of the  $\chi$ SB QNMs:  $\mathcal{B}_{3u}$ ,  $\mathcal{B}_{3s}$  and  $\mathcal{B}_7$ . We find that the former two branches in the limit  $T \gg \Lambda$  combine into a single branch representing  $\Delta = 3$  QNMs of the  $AdS_5$ -Schwarzschild black hole [18]. At high temperatures, the degeneracy between the two branches is broken by  $\mathcal{O}(1/\sqrt{\ln \frac{T}{\Lambda}})$  effects. Following these branches to low temperatures, we recover the instability on the  $\mathcal{B}_{3u}$  branch at  $T_{\chi SB}$  (1.1), originally found in [2]. The other branch,  $\mathcal{B}_{3s}$ , corresponds to the QNMs that remain stable for  $T > T_{\chi SB}$ . The  $\mathcal{B}_7$  branch at high temperatures represents  $\Delta = 7$  QNMs of the  $AdS_5$ -Schwarzschild black hole [18]. The dispersion relation of its QNMs differ from that of the conformal modes by  $\mathcal{O}(1/\ln \frac{T}{\Lambda})$  effects. Similar to the  $\mathcal{B}_{3s}$  branch, the  $\mathcal{B}_7$  branch corresponds to the QNMs that remain stable for  $T > T_{\chi SB}$ . Thus, we conclude that the  $\chi$ SB instability of [2] is the dominant perturbative instability of the Klebanov-Tseytlin black hole for  $T \geq T_{\chi SB}$ . Of course, this is the instability of the lowest QNM on the  $\mathcal{B}_{3u}$  branch — as one further reduces the temperature below  $T_{\chi SB}$ , one expects developing instabilities of the excited QNMs

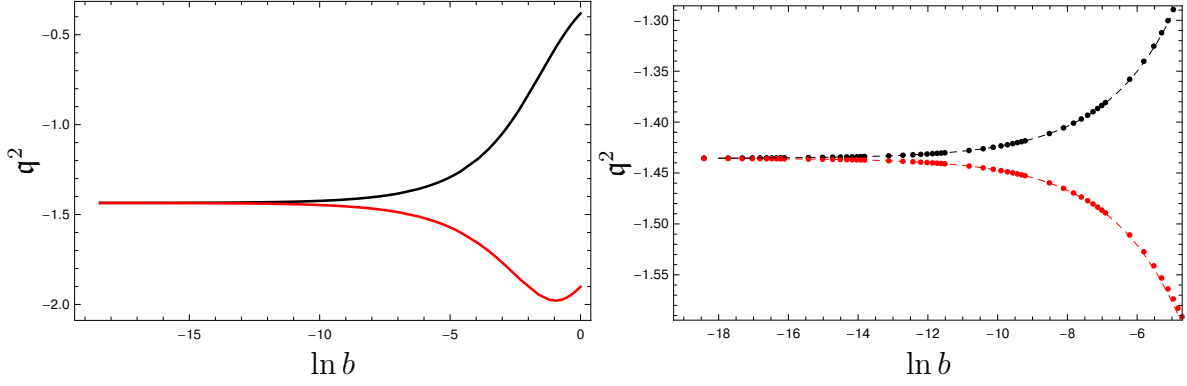


Figure 1: Functional dependence of  $q^2 \equiv k^2/(2\pi T)^2$  of the quasinormal modes of the  $\mathcal{B}_{3u}$  branch (black) and of the quasinormal modes of the  $\mathcal{B}_{3s}$  branch (red) at  $\omega = 0$  in the high-temperature/small  $b$  (see (1.4)) regime of the KT black hole. These quasinormal modes are dual to the fluctuations of the  $\chi$ SB gaugino condensate operators in the symmetric phase of the cascading gauge theory plasma. The dashed curves in the right panel show the leading order high-temperature corrections to the conformal value of  $q^2$  — a temperature independent result for the quasinormal mode dual to the dimension-3 operator in the holographic  $CFT_4$ . The QNMs are stable since  $q^2 < 0$ , in the temperature regime reported.

on  $\mathcal{B}_{3u}$ , as well as on the other two branches of the  $\chi$ SB sector.

In the rest of this section we present the numerical results for the spectrum of the QNMs on the three branches of the  $\chi$ SB sector. Specifically, we analyze  $q^2 \equiv k^2/(2\pi T)^2$  of the QNMs at zero frequency,  $\omega = 0$ , as one varies the Hawking temperature of the KT black hole. A QNM becomes unstable once  $q^2 > 0$ . The technical details relevant to the reported results are collected in section 2 and the appendices A and B. In section 3 we present an independent argument for the absence of the KS black holes (in addition to the one constructed in [1]), perturbatively related to the KT black hole.

Figs. 1 and 2 present the results for the  $q^2$  (dimensionless momentum, see (2.39)) of the lowest QNMs for the three branches  $\mathcal{B}_{3u}$  (black curves),  $\mathcal{B}_{3s}$  (red curves) and  $\mathcal{B}_7$  (green curves) at zero frequency  $\omega = 0$  and high temperature, see section 2.3. In the limit  $b \rightarrow 0$ ,

$$\ln b \approx -\ln \left( 2 \ln \frac{T}{\Lambda} \right). \quad (1.4)$$

The fact that  $q^2 < 0$  for all the QNMs implies that the chiral symmetry breaking

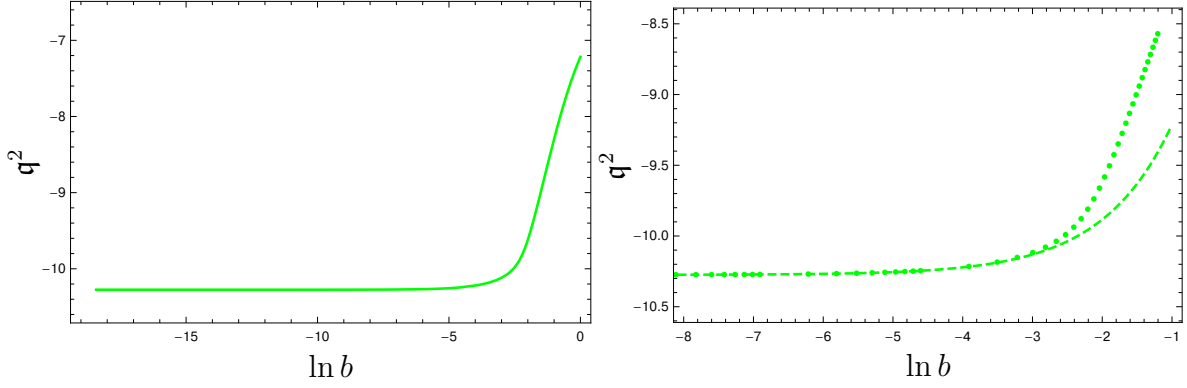


Figure 2: Functional dependence of  $\mathfrak{q}^2 \equiv k^2/(2\pi T)^2$  of the quasinormal modes of the  $\mathcal{B}_7$  branch at  $\omega = 0$  in the high-temperature/small  $b$  (see (1.4)) regime of the KT black hole. These quasinormal modes are dual to the fluctuations of the  $\chi$ SB dimension-7 operator in the symmetric phase of the cascading gauge theory plasma. The dashed curve in the right panel shows the leading order high-temperature correction to the conformal value of  $\mathfrak{q}^2$  — a temperature independent result for the quasinormal mode dual to the dimension-7 operator in the holographic  $CFT_4$ . The QNMs are stable since  $\mathfrak{q}^2 < 0$ , in the temperature regime reported.

fluctuations in the KT black hole are massive, and exponentially decay both in time and space when excited. The dashed curves in the right panels indicate the values of  $\mathfrak{q}^2$  for the corresponding QNM branch in the conformal limit, along with the leading order corrections:  $\mathcal{O}(b)$  of (A.13) for the  $\mathcal{B}_7$  branch, and  $\mathcal{O}(\sqrt{b})$  for the  $\mathcal{B}_{3u}$  (plus sign in (B.16)) and  $\mathcal{B}_{3s}$  (minus sign in (B.16)).

In fig. 3 we follow the QNM branch  $\mathcal{B}_{3u}$  to low temperatures. The results reported reproduce the analysis presented in [2]. We perform analysis in two computation schemes (see section 2.2): SchemeA (the solid blue curve) and SchemeB (the solid black curves). The solid black curve data is the low temperature extension of the data presented in fig. 1 (also the solid black curve in the left panel and the black dots in the right panel). There is an excellent agreement between the two computational schemes in the overlapping regime (overlapping black and blue curves in the left panel) — the fractional difference in the results is at the level  $\propto 10^{-6}$ . The solid blue curve (in both panels) crosses  $\mathfrak{q}^2 = 0$  at the location highlighted by the vertical dashed blue line, indicating the instability of the lowest QNM on the  $\mathcal{B}_{3u}$  branch. This occurs precisely at the  $\chi$ SB phase transition (1.1), as found in [2]. The vertical dashed red

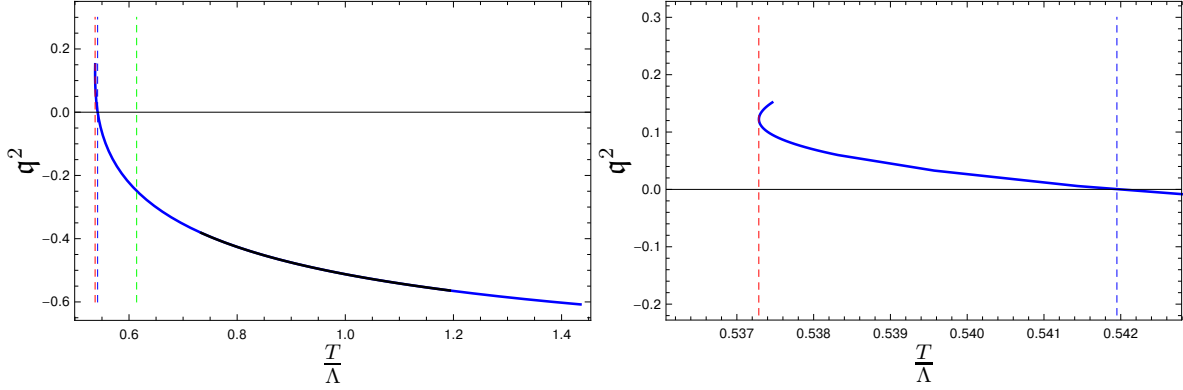


Figure 3:  $q^2$  of the lowest QNM on the  $\mathcal{B}_{3u}$  branch as a function of  $\frac{T}{\Lambda}$ .  $q^2 > 0$  for  $T < T_{\chi\text{SB}}$  (the vertical dashed blue lines), signaling the perturbative instability. The blue curve represents the results in the computational SchemeA, and the black curve represents the results in the computational SchemeB (the low-temperature extension of the data presented in fig. 1). The vertical dashed red lines indicate the terminal temperature of the KT black hole,  $T_u$  (1.3). The vertical green dashed line indicates the temperature of the first-order confinement phase transition for the KT black hole,  $T_c$  (1.2).

lines highlight the temperature  $T_u$  (1.3), and the vertical green dashed line highlights the temperature  $T_c$  of the confinement phase transition, see (1.2).

In fig. 4 we follow the QNM branches  $\mathcal{B}_{3s}$  (the left panel) and  $\mathcal{B}_7$  (the right panel) to low temperatures. The results reported are new. There are no instabilities on either branch for  $T > T_{\chi\text{SB}}$  (the vertical dashed blue lines). The horizontal black lines indicate  $q^2(T_{\chi\text{SB}}/\Lambda)$  for the corresponding branch. The vertical green dashed lines highlight  $T_c/\Lambda$ . The solid orange and magenta curves are computed in SchemeA, while the solid red and green curves are computed in SchemeB. As for the branch  $\mathcal{B}_{3u}$ , the fractional differences in the results from the different schemes is at the level  $\propto 10^{-6}$ .

## 2 Effective action, equations of motion and the boundary asymptotes for $\chi\text{SB}$ QNMs of the KT black hole

The five-dimensional effective action (KS) describing  $SU(2) \times SU(2) \times \mathbb{Z}_2$  states of the cascading gauge theory has been derived in [2]. This effective action contains as an on-shell solution the Klebanov-Strassler black hole constructed in [1]. The KS

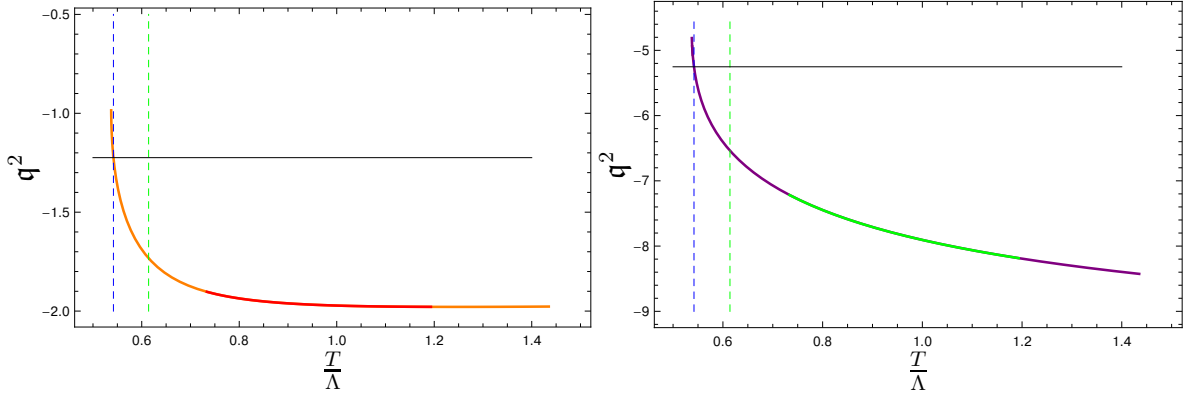


Figure 4:  $q^2$  of the lowest QNMs on the  $\mathcal{B}_{3s}$  branch (the left panel) and on the  $\mathcal{B}_7$  branch (the right panel) as a function of  $\frac{T}{\Lambda}$ .  $q^2 < 0$  for  $T > T_{\chi SB}$  (the vertical dashed blue lines), indicating that these QNMs are stable in the temperature regime indicated. The orange/magenta curves represent the results in the computational SchemeA, and the red/green curves represent the results in the computational SchemeB (the low-temperature extensions of the data presented in figs. 1 and 2). The vertical green dashed lines indicate the temperature of the first-order confinement phase transition for the KT black hole,  $T_c$  (1.2). The horizontal black lines denote  $q^2(T_{\chi SB}/\Lambda)$  for the lowest QNM on the corresponding branch.

effective action allows for a consistent truncation to a  $U(1)$  chirally symmetric sector, reproducing the Klebanov-Tseytlin (KT) effective action [9]. The KT effective action contains as an on-shell solution the KT black hole, constructed<sup>4</sup> in [3]. The effective action for the chiral symmetry breaking sector, *i.e.*, for the  $U(1)$  chiral symmetry breaking linearized fluctuations on top of the KT states of the cascading gauge theory, was derived in [2]. Only one branch (out of the total three branches) of the QNMs was identified and analyzed in [2]. The QNM instability found in [2] identified a bifurcation point for a branch of the Klebanov-Strassler black holes, perturbatively connected to the KT black hole. In this section we review the relevant effective actions, the equations of motion, and the boundary asymptotes for the  $\chi SB$  QNMs of the KT black hole. Next, we proceed to a careful analysis of the QNMs in the conformal (or high-temperature) limit,  $P^2 \rightarrow 0$ . Although it is straightforward to identify the three branches of the QNMs (two for the operators of  $\Delta = 3$  and a single one for the operator of  $\Delta = 7$ ) in the strict  $P^2 = 0$  (conformal) limit, constructing perturbative

<sup>4</sup>The KT black hole at high temperatures (near conformal limit) was discussed in [6–8, 13].



in  $P^2$  expansions for  $\Delta = 3$  branches is rather subtle: while the KT BH is a series expansion<sup>5</sup> in  $P^2$  of the  $AdS_5$  Schwarzschild black hole, we find here that the pair of  $\Delta = 3$  QNM branches realize a series expansion<sup>6</sup> in  $\sqrt{P^2}$  — the appearance of the square root branch point, *i.e.*,  $\pm\sqrt{P^2}$ , naturally leads to breaking of the spectral degeneracy in the two  $\Delta = 3$  QNM branches at finite  $P^2$ . Once the QNM branches are constructed in the high-temperature (conformal) limit, it is straightforward to follow them to low-temperatures. These results are reported in section 1: see figs. 1-4.

## 2.1 The effective actions

The effective gravitational action describing  $SU(2) \times SU(2) \times \mathbb{Z}_2$  states of the cascading gauge theory is given by [2]

$$\begin{aligned}
S_5 = & \frac{108}{16\pi G_5} \int_{\mathcal{M}_5} \text{vol}_{\mathcal{M}_5} \Omega_1 \Omega_2^2 \Omega_3^2 \left\{ R_{10} - \frac{1}{2} (\nabla \Phi)^2 \right. \\
& - \frac{1}{2} e^{-\Phi} \left( \frac{(h_1 - h_3)^2}{2\Omega_1^2 \Omega_2^2 \Omega_3^2} + \frac{1}{\Omega_3^4} (\nabla h_1)^2 + \frac{1}{\Omega_2^4} (\nabla h_3)^2 \right) \\
& - \frac{1}{2} e^{\Phi} \left( \frac{2}{\Omega_2^2 \Omega_3^2} (\nabla h_2)^2 + \frac{1}{\Omega_1^2 \Omega_2^4} \left( h_2 - \frac{P}{9} \right)^2 + \frac{1}{\Omega_1^2 \Omega_3^4} h_2^2 \right) \\
& \left. - \frac{1}{2\Omega_1^2 \Omega_2^4 \Omega_3^4} \left( 4\Omega_0 + h_2 (h_3 - h_1) + \frac{1}{9} P h_1 \right)^2 \right\}, \tag{2.1}
\end{aligned}$$

where

$$\begin{aligned}
R_{10} = & R_5 + \left( \frac{1}{2\Omega_1^2} + \frac{2}{\Omega_2^2} + \frac{2}{\Omega_3^2} - \frac{\Omega_2^2}{4\Omega_1^2 \Omega_3^2} - \frac{\Omega_3^2}{4\Omega_1^2 \Omega_2^2} - \frac{\Omega_1^2}{\Omega_2^2 \Omega_3^2} \right) - 2\Box \ln (\Omega_1 \Omega_2^2 \Omega_3^2) \\
& - \left\{ (\nabla \ln \Omega_1)^2 + 2 (\nabla \ln \Omega_2)^2 + 2 (\nabla \ln \Omega_3)^2 + (\nabla \ln (\Omega_1 \Omega_2^2 \Omega_3^2))^2 \right\}, \tag{2.2}
\end{aligned}$$

is the Ricci scalar of the ten-dimensional background geometry

$$ds_{10}^2 = g_{\mu\nu}(y) dy^\mu dy^\nu + \Omega_1^2(y) g_5^2 + \Omega_2^2(y) [g_3^2 + g_4^2] + \Omega_3^2(y) [g_1^2 + g_2^2], \tag{2.3}$$

with the one-forms  $g_i$  are the usual forms of the  $T^{1,1}$  (see [2] for explicit expressions), and  $R_5$  is the five-dimensional Ricci scalar of

$$ds_5^2 = g_{\mu\nu}(y) dy^\mu dy^\nu. \tag{2.4}$$

---

<sup>5</sup>See [13] for the KT black hole construction up to  $\mathcal{O}(P^8)$  inclusive.

<sup>6</sup>The same phenomenon was observed also for the normal modes of the  $\chi$ SB sector of the cascading gauge theory vacuum on  $S^3$  in [19].

The scalars  $h_i = h_i(y)$  parameterize the three forms fluxes,  $\Phi = \Phi(y)$  is the dilaton and the constant<sup>7</sup>  $\Omega_0$  determine the five-form flux (see [2] for the details). Parameter  $P$  must be appropriately quantized [4],

$$P = \frac{9}{2} M \alpha', \quad (2.5)$$

corresponding to the integer  $M$ , *i.e.*, the difference of the ranks of the cascading gauge theory gauge group factors. Finally,  $G_5$  is the five dimensional effective gravitational constant

$$G_5 \equiv \frac{G_{10}}{\text{vol}_{T^{1,1}}} = \frac{27}{16\pi^3} G_{10}, \quad (2.6)$$

where  $16\pi G_{10} = (2\pi)^7 (\alpha')^4$  is 10-dimensional gravitational constant of type IIB supergravity.

In what follows we introduce

$$\begin{aligned} h_1 &= \frac{1}{P} \left( \frac{K_1}{12} - 36\Omega_0 \right), & h_2 &= \frac{P}{18} K_2, & h_3 &= \frac{1}{P} \left( \frac{K_3}{12} - 36\Omega_0 \right), \\ \Omega_1 &= \frac{1}{3} f_c^{1/2} h^{1/4}, & \Omega_2 &= \frac{1}{\sqrt{6}} f_a^{1/2} h^{1/4}, & \Omega_3 &= \frac{1}{\sqrt{6}} f_b^{1/2} h^{1/4}, & g &= e^\Phi. \end{aligned} \quad (2.7)$$

Chirally symmetric states of the cascading gauge theory correspond to the enhancement of the global symmetry  $SU(2) \times SU(2) \times \mathbb{Z}_2 \rightarrow SU(2) \times SU(2) \times U(1)$ , and are described by the gravitational configurations of (2.1) subject to the constraints<sup>8</sup>:

$$h_1 = h_3, \quad h_2 = \frac{P}{18}, \quad \Omega_2 = \Omega_3. \quad (2.8)$$

The chiral symmetry breaking sector is parameterized by  $\{\delta f, \delta k_1, \delta k_2\}$  in

$$\begin{aligned} K_1 &= K + \delta k_1, & K_2 &= 1 + \delta k_2, & K_3 &= K - \delta k_1, \\ f_c &= f_2, & f_a &= f_3 + \delta f, & f_b &= f_3 - \delta f. \end{aligned} \quad (2.9)$$

Its linearized fluctuations on top of the  $U(1)$ -symmetric on-shell backgrounds

$$\left\{ ds_5^2, K, h, f_2, f_3, g \right\} \quad (2.10)$$

---

<sup>7</sup>In the limit of the vanishing 3-form fluxes,  $\Omega_0 = \frac{L^4}{108}$ , where  $L$  is the asymptotic  $AdS_5$  radius.

<sup>8</sup>This is a consistent truncation of the cascading gauge theory to  $U(1)$  symmetric sector constructed in [9].

are governed by the following effective action<sup>9</sup> [2]

$$S_{\chi\text{SB}}[\delta f, \delta k_1, \delta k_2] = \frac{1}{16\pi G_5} \int_{\mathcal{M}_5} \text{vol}_{\mathcal{M}_5} h^{5/4} f_2^{1/2} f_3^2 \left\{ \mathcal{L}_1 + \mathcal{L}_2 + \mathcal{L}_3 + \mathcal{L}_4 + \mathcal{L}_5 \right\}, \quad (2.11)$$

$$\mathcal{L}_1 = -\frac{(\delta f)^2}{f_3^2} \left( -\frac{P^2 e^\Phi}{2f_2 h^{3/2} f_3^2} - \frac{(\nabla K)^2}{8f_3^2 h P^2 e^\Phi} - \frac{K^2}{2f_2 h^{5/2} f_3^4} \right), \quad (2.12)$$

$$\begin{aligned} \mathcal{L}_2 = & -\frac{9f_3^2 - 24f_2 f_3 + 4f_2^2}{f_2 h^{1/2} f_3^4} (\delta f)^2 + 2\Box \frac{(\delta f)^2}{f_3^2} - \left( \nabla \frac{(\delta f)^2}{f_3^2} \right)^2 \\ & - 2\nabla \left( \ln h^{1/4} f_3^{1/2} \right) \nabla \left( \frac{(\delta f)^2}{f_3^2} \right) + 2\nabla \left( \ln f_2^{1/2} h^{5/4} f_3^2 \right) \nabla \left( \frac{(\delta f)^2}{f_3^2} \right), \end{aligned} \quad (2.13)$$

$$\begin{aligned} \mathcal{L}_3 = & -\frac{1}{2P^2 e^\Phi} \left( \frac{9}{2f_2 h^{3/2} f_3^2} (\delta k_1)^2 + \frac{1}{2h f_3^4} \left( 2(\nabla K)^2 (\delta f)^2 + f_3^2 (\nabla \delta k_1)^2 \right. \right. \\ & \left. \left. + 4f_3 \delta f \nabla K \nabla \delta k_1 \right) \right), \end{aligned} \quad (2.14)$$

$$\mathcal{L}_4 = \frac{P^2 e^\Phi}{2} \left( \frac{2}{9h f_3^2} (\nabla \delta k_2)^2 + \frac{2}{f_2 h^{3/2} f_3^4} (3(\delta f)^2 + 4f_3 \delta f \delta k_2 + f_3^3 (\delta k_2)^2) \right), \quad (2.15)$$

$$\mathcal{L}_5 = \frac{K}{f_2 h^{5/2} f_3^6} (f_3^2 \delta k_1 \delta k_2 - K (\delta f)^2). \quad (2.16)$$

## 2.2 KT black hole and $\chi\text{SB}$ quasinormal modes

The Klebanov-Tseytlin black hole [3] is a chirally symmetric (see (2.8)) solution of the effective action (2.1). The five-dimensional metric is

$$ds_5^2 = h^{-1/2} (2x - x^2)^{-1/2} \left( -(1-x)^2 dt^2 + dx_1^2 + dx_2^2 + dx_3^2 \right) + G_{xx} dx^2, \quad (2.17)$$

where

$$\begin{aligned} G_{xx} = & \frac{\sqrt{h} f_3^2}{2(x-1)P^2 g^2 (2-x)^2 x^2 (K^2 + 8h^2 f_3^2 f_2 (f_2 - 6f_3) + 2h f_3^2 P^2 g)} \left( 12P^2 f_3^2 g^2 f_2 h^2 \right. \\ & \times (1-x) + f_2 x^2 (2P^2 f_3^2 g^2 h'^2 - 12P^2 g^2 h^2 f_3'^2 + K'^2 h g + 2P^2 h^2 f_3^2 g'^2) (x-1)(2-x)^2 \\ & - 4xP^2 f_3 g^2 h f_2 (2-x)(x^2 - 2x + 2)(h' f_3 + 4f_3' h) + 4xP^2 f_3 (2-x)g^2 h^2 \\ & \left. \times (2x f_3' (1-x)(2-x) - (x^2 - 2x + 2)f_3) f_2' \right). \end{aligned} \quad (2.18)$$

---

<sup>9</sup>Since the fluctuations  $\{\delta f, \delta k_1, \delta k_2\}$  break the chiral  $U(1)$  symmetry to  $\mathbb{Z}_2$ , they can never mix with any  $U(1)$ -symmetric fluctuations of the background (2.10). This was also verified explicitly in the analysis reported in [2], both from the effective action perspective, and from the perspective of the second-order equations of motion of the KS black hole.

The gravitational bulk scalars<sup>10</sup>  $\{K, h, f_2, f_3, g\}$  are functions of the radial coordinate  $x \in (0, 1)$ . Asymptotically near the boundary ( $x \rightarrow 0_+$ ),

$$K = P^2 g_0 \left[ k_s - \frac{1}{2} \ln x + \sum_{n=1}^{\infty} \sum_k K_{n,k} x^{n/2} \ln^k x \right], \quad (2.19)$$

$$h = \frac{P^2 g_0}{a_0^2} \left[ \frac{1}{8} + \frac{k_s}{4} - \frac{1}{8} \ln x + \sum_{n=1}^{\infty} \sum_k h_{n,k} x^{n/2} \ln^k x \right], \quad (2.20)$$

$$f_2 = a_0 \left[ 1 + \sum_{n=1}^{\infty} \sum_k f_{2,n,k} x^{n/2} \ln^k x \right], \quad (2.21)$$

$$f_3 = a_0 \left[ 1 + \sum_{n=1}^{\infty} \sum_k f_{3,n,k} x^{n/2} \ln^k x \right], \quad (2.22)$$

$$g = g_0 \left[ 1 + \sum_{n=1}^{\infty} \sum_k g_{n,k} x^{n/2} \ln^k x \right], \quad (2.23)$$

characterized by  $\{f_{3,2,0}, f_{3,3,0}, f_{3,4,0}, g_{2,0}\}$  (in addition to  $P, g_0, a_0$ ); while near the horizon ( $y \equiv 1 - x \rightarrow 0_+$ ),

$$\begin{aligned} K &= P^2 g_0 \sum_{n=0}^{\infty} k_n^h y^{2n}, & h &= \frac{P^2 g_0}{a_0^2} \sum_{n=0}^{\infty} h_n^h y^{2n}, & f_2 &= a_0 \sum_{n=0}^{\infty} f_{2,n}^h y^{2n}, \\ f_3 &= a_0 \sum_{n=0}^{\infty} f_{3,n}^h y^{2n}, & g &= g_0 \sum_{n=0}^{\infty} g_n^h y^{2n}, \end{aligned} \quad (2.24)$$

completely specified with  $\{k_0^h, h_0^h, f_{2,0}^h, f_{3,0}^h, f_{3,1}^h, g_0^h\}$ . The thermodynamics of the KT black hole was discussed in [3]; in what follows we will need only the expression for the Hawking temperature and the strong coupling scale of the theory, see [3, 10],

$$T = \sqrt{\frac{a_0}{P^2 g_0}} \times \sqrt{\frac{3f_{3,0}^h - f_{2,0}^h}{2\pi^2 f_{3,0}^h h_0^h (f_{3,0}^h + 2f_{3,1}^h)}}, \quad \Lambda = \frac{\sqrt{a_0}}{P^2 g_0} e^{-k_s/2}. \quad (2.25)$$

Using the KT background (2.17), and the plane-wave ansatz for the chiral symmetry breaking fluctuations,

$$\delta f = e^{-i\omega t + ikx_3} F, \quad \delta k_1 = e^{-i\omega t + ikx_3} \mathcal{K}_1, \quad \delta k_2 = e^{-i\omega t + ikx_3} \mathcal{K}_2, \quad (2.26)$$

---

<sup>10</sup>See eq.(2.8)-(2.12) of [3] for the corresponding equations of motion.

we find from (2.11) the equations of motion for the QNM wavefunctions  $\{F, \mathcal{K}_1, \mathcal{K}_2\}$ , all of them being the functions of the radial coordinate  $x$ ,

$$0 = F'' - \left( \frac{2f_3}{f_3} + \frac{1}{1-x} \right) F' - \frac{K'}{2hP^2gf_3} \mathcal{K}_1' - \frac{2gP^2G_{xx}}{h^{3/2}f_3f_2} \mathcal{K}_2 + \left( \frac{(f_3')^2}{f_3^2} - \frac{(K')^2}{2ghf_3^2P^2} \right. \\ \left. + \left[ h^{1/2}\sqrt{2x-x^2} \left( \frac{\omega^2}{(1-x)^2} - k^2 \right) + \frac{4hf_2^2 - 9hf_3^2 - 2gP^2}{f_3^2f_2h^{3/2}} \right] G_{xx} + \frac{2}{(2x-x^2)^2} \right) F, \quad (2.27)$$

$$0 = \mathcal{K}_1'' - \left( \frac{2f_3'}{f_3} + \frac{h'}{h} + \frac{g'}{g} + \frac{1}{1-x} \right) \mathcal{K}_1' + \frac{2K'}{f_3} F' + \frac{2KgP^2G_{xx}}{f_3^2f_2h^{3/2}} \mathcal{K}_2 + \left( \frac{4KgP^2G_{xx}}{h^{3/2}f_2f_3^3} \right. \\ \left. - \frac{2f_3'K'}{f_3^2} \right) F + \left[ h^{1/2}\sqrt{2x-x^2} \left( \frac{\omega^2}{(1-x)^2} - k^2 \right) - \frac{9}{h^{1/2}f_2} \right] G_{xx} \mathcal{K}_1, \quad (2.28)$$

$$0 = \mathcal{K}_2'' - \left( \frac{2f_3'}{f_3} + \frac{h'}{h} - \frac{g'}{g} + \frac{1}{1-x} \right) \mathcal{K}_2' + \left[ h^{1/2}\sqrt{2x-x^2} \left( \frac{\omega^2}{(1-x)^2} - k^2 \right) - \frac{9}{h^{1/2}f_2} \right] \\ \times G_{xx} \mathcal{K}_2 - \frac{18G_{xx}}{h^{1/2}f_3f_2} F + \frac{9KG_{xx}}{2h^{3/2}gf_2f_3^2P^2} \mathcal{K}_1. \quad (2.29)$$

To determine the spectrum of the QNMs, one needs to solve (2.27)-(2.29) with “normalizable only” conditions at the bulk gravitational boundary, and the incoming-wave boundary conditions are the horizon [20]. Fixing (without the loss of generality) the normalizable coefficient of  $F$  to one, see (2.36) below, the above boundary conditions determine the spectrum of the QNMs:

$$\omega = \omega \left( q \equiv k^2, \frac{T}{\Lambda} \right). \quad (2.30)$$

As in [2], we are not interested in the numerical data for the spectrum per se, rather, we would like to identify QNMs at the threshold of instability. To this end, we solve

$$0 = \omega \left( q, \frac{T}{\Lambda} \right) \Big|_{q=\frac{a_0}{P^2g_0} \hat{q}} \implies \hat{q} = \hat{q} \left( \frac{T}{\Lambda} \right), \quad (2.31)$$

where we introduced the dimensionless  $\hat{q}$ . The KT black hole is unstable with respect to the chiral symmetry breaking fluctuations for all temperatures  $T$  such that  $\hat{q} > 0$  [2], *i.e.*,

$$\hat{q} > 0 \iff \text{KT black hole } \chi\text{SB perturbative instability} \quad (2.32)$$

Focusing on the instability criteria (2.31), the asymptotic expansions for the linearized  $\chi$ SB fluctuations take form:

■ in the UV, *i.e.*, as  $x \rightarrow 0_+$ ,

$$F = a_0 x^{3/4} \left( f_{3,0} + x^{1/2} \left( -\frac{\sqrt{2}}{32} \hat{q} f_{3,0} \ln x + \frac{\sqrt{2}}{96} \hat{q} (3f_{3,0} k_s + 13f_{3,0} - 2k_{2,3,0}) \right) + \mathcal{O}(x \ln^2 x) \right), \quad (2.33)$$

$$\begin{aligned} \mathcal{K}_1 = P^2 g_0 x^{3/4} & \left( \frac{1}{2} f_{3,0} \ln x + \frac{2}{3} f_{3,0} + \frac{2}{3} k_{2,3,0} + x^{1/2} \left( -\frac{\sqrt{2}}{128} \hat{q} f_{3,0} \ln^2 x + \frac{\sqrt{2}}{192} \hat{q} (3f_{3,0} k_s \right. \right. \\ & \left. \left. + f_{3,0} - 2k_{2,3,0}) \ln x - \frac{\sqrt{2}}{384} \hat{q} (f_{3,0} k_s - 8k_{2,3,0} k_s - 56f_{3,0} - 2k_{2,3,0}) \right) + \mathcal{O}(x \ln^3 x) \right), \end{aligned} \quad (2.34)$$

$$\begin{aligned} \mathcal{K}_2 = x^{3/4} & \left( \frac{3}{4} f_{3,0} \ln x + k_{2,3,0} + x^{1/2} \left( -\frac{3\sqrt{2}}{256} \hat{q} f_{3,0} \ln^2 x + \frac{\sqrt{2}}{128} \hat{q} (3f_{3,0} k_s + 3f_{3,0} - 2k_{2,3,0}) \right. \right. \\ & \left. \left. \times \ln x + \frac{\sqrt{2}}{640} \left( -\frac{15}{2} \hat{q} k_s f_{3,0} + 20k_{2,3,0} k_s \hat{q} + 75\hat{q} f_{3,0} + 15k_{2,3,0} \hat{q} \right) \right) \right. \\ & \left. + x \left( k_{2,7,0} + \dots + \mathcal{O}(\ln^3 x) \right) + \mathcal{O}(x^{3/2} \ln^4 x) \right), \end{aligned} \quad (2.35)$$

characterized by (we fixed the overall normalization of the linearized fluctuations setting the normalizable coefficient of  $F$ )

$$\{f_{3,0} = 1, k_{2,3,0}, k_{2,7,0}, \hat{q}\}; \quad (2.36)$$

■ in the IR, *i.e.*, as  $y = 1 - x \rightarrow 0_+$ ,

$$F = a_0 \left( F_0^h + \mathcal{O}(y^2) \right), \quad \mathcal{K}_1 = P^2 g_0 \left( K_{1,0}^h + \mathcal{O}(y^2) \right), \quad \mathcal{K}_2 = K_{2,0}^h + \mathcal{O}(y^2), \quad (2.37)$$

characterized (in addition to  $\hat{q}$ ) by

$$\{F_0^h, K_{1,0}^h, K_{2,0}^h\}. \quad (2.38)$$

Given a KT black hole solution at a certain temperature, we expect three distinct branches of the quasinormal modes — the  $\chi$ SB sector mixes in three gravitational modes  $\{\delta f, \delta k_1, \delta k_2\}$ , dual to a pair of dimension  $\Delta = 3$  operators (the normalizable

coefficients  $f_{3,0}$  and  $k_{2,3,0}$ ), and a single dimension  $\Delta = 7$  operator (the normalizable coefficient  $k_{2,7,0}$ ). Furthermore, each QNM branch has its own tower of excitations, with increasingly higher  $\hat{q}$ , characterized by the number of nodes in the radial wavefunction. In section 2.3 we identify each QNM branch at high temperatures, where particular linear combinations of  $\{\delta f, \delta k_1, \delta k_2\}$  decouple. We then follow the lowest QNM of each branch numerically to low temperatures. We employ two different computational schemes: SchemeA and SchemeB.

- SchemeA: as in [2], we set  $P = a_0 = g_0 = 1$  as vary  $k_s$  — this is a convenient regime to reach low temperatures.
- SchemeB: alternatively, we set  $a_0 = g_0 = 1$  and  $k_s = \frac{1}{b}$ ,  $P^2 = b$  — this is a convenient regime to reach high temperatures.

Results of these computations are collected in Figs. 1-4. We plot dimensionless quantities:

$$\mathfrak{q}^2 \equiv \frac{k^2}{(2\pi T)^2} = \frac{q}{(2\pi T)^2} = \frac{a_0}{P^2 g_0} \times \frac{\hat{q}}{(2\pi T)^2} = \hat{q} \frac{f_{3,0}^h h_0^h (f_{3,0}^h + 2f_{3,1}^h)}{2(3f_{3,0}^h - f_{2,0}^h)}, \quad (2.39)$$

as a function of

$$\frac{T}{\Lambda} = \sqrt{P^2 g_0} e^{ks/2} \sqrt{\frac{3f_{3,0}^h - f_{2,0}^h}{2\pi^2 f_{3,0}^h h_0^h (f_{3,0}^h + 2f_{3,1}^h)}}, \quad (2.40)$$

in the computational SchemeA, or as a function of  $b$  in the computational SchemeB.

### 2.3 High-temperature (near-conformal) limit

There are three branches of the quasinormal modes associated with the  $\chi$ SB sector of the cascading gauge theory. In this section we explain how these branches are identified by the decoupled linear combinations of the  $\chi$ SB fluctuations  $\{\delta f, \delta k_1, \delta k_2\}$  in the KT black hole background at high temperatures. We use the computational SchemeB (see section 2.3), *i.e.*, the KT black hole in the near conformal  $b \rightarrow 0$  limit.

Exactly at  $b = 0$  the KT BH is just the  $AdS_5$ -Schwarzschild black hole:

$$h \equiv \frac{1}{4}, \quad K \equiv 1, \quad f_2 = f_3 \equiv 1, \quad g \equiv 1, \quad (2.41)$$

where the  $AdS_5$  radius is

$$L^4 = \frac{1}{4}. \quad (2.42)$$

The leading order  $\mathcal{O}(b)$  corrections were discussed in [8]; here we follow the state-of-the-art construction of [13], done to  $\mathcal{O}(b^4)$  inclusive:

$$\begin{aligned}
h(x) &= \frac{1}{4} + \sum_{n=1}^{\infty} \left\{ b^n \left( \xi_{2n}(x) - \frac{5}{4} \eta_{2n}(x) \right) \right\}, \\
f_2(x) &= 1 + \sum_{n=1}^{\infty} \left\{ b^n \left( -2\xi_{2n}(x) + \eta_{2n}(x) + \frac{4}{5} \lambda_{2n}(x) \right) \right\}, \\
f_3(x) &= 1 + \sum_{n=1}^{\infty} \left\{ b^n \left( -2\xi_{2n}(x) + \eta_{2n}(x) - \frac{1}{5} \lambda_{2n}(x) \right) \right\}, \\
K(x) &= 1 + \sum_{n=1}^{\infty} \left\{ b^n \kappa_{2n}(x) \right\}, \\
g(x) &= 1 + \sum_{n=1}^{\infty} \left\{ b^n \zeta_{2n}(x) \right\}.
\end{aligned} \tag{2.43}$$

The equations for  $\{\kappa_{2n}, \xi_{2n}, \eta_{2n}, \lambda_{2n}, \zeta_{2n}\}$  decouple at each order  $n$ , see eqs. (2.16)-(2.20) of [13]. At order  $n = 1$ ,  $\kappa_2$  and  $\xi_2$  can be determined analytically<sup>11</sup>:

$$\kappa_2 = -\frac{1}{2} \ln x - \frac{1}{2} \ln \left( 1 - \frac{1}{2}x \right), \quad \xi_2 = \frac{1}{12}(\ln x - 1) + \frac{1}{12} \ln \left( 1 - \frac{1}{2}x \right), \tag{2.44}$$

while the remaining functions  $\eta_2, \lambda_2, \zeta_2$  has to be determined numerically. We will need the asymptotes of these functions:

■ in the UV, *i.e.*, as  $x \rightarrow 0_+$ ,

$$\begin{aligned}
\eta_2 &= \frac{1}{6} \ln x - \frac{1}{6} - \frac{x}{30} + x^2 \left( \eta_{2,2,0} + \frac{1}{30} \ln x \right) + \mathcal{O}(x^3 \ln x), \\
\lambda_2 &= \frac{2}{3}x + \lambda_{2,3}x^{3/2} + \mathcal{O}(x^2), \quad \zeta_2 = x \left( \frac{1}{2} \ln x + \zeta_{2,1,0} \right) + \mathcal{O}(x^2 \ln x);
\end{aligned} \tag{2.45}$$

■ in the IR, *i.e.*, as  $y = 1 - x \rightarrow 0_+$ ,

$$\begin{aligned}
\eta_2 &= \eta_{2,0}^h + \left( \frac{7}{60} + \frac{1}{3} \ln 2 + 2\eta_{2,0}^h \right) y^2 + \mathcal{O}(y^4), \\
\lambda_2 &= \lambda_{2,0}^h + \left( \frac{3}{4} \lambda_{2,0}^h - \frac{1}{4} \right) y^2 + \mathcal{O}(y^4), \quad \zeta_2 = \zeta_{2,0}^h + \frac{1}{4} y^2 + \mathcal{O}(y^4).
\end{aligned} \tag{2.46}$$

To order  $\mathcal{O}(b)$  the Hawking temperature of the KT black hole can be computed analytically,

$$2\pi T = 4 - (1 + \ln 2)b + \mathcal{O}(b^2), \tag{2.47}$$

---

<sup>11</sup>Any free integration constants are fixed so to enforce the computational SchemeB.



additionally, from (2.40),

$$\frac{1}{b} + \mathcal{O}(\ln b) = 2 \ln \frac{T}{\Lambda}. \quad (2.48)$$

Assuming, at fixed  $\omega$ ,

$$\begin{aligned} F(x) &= \sum_{n=1}^{\infty} \left\{ b^{n/2} F_n(x) \right\}, \\ \mathcal{K}_1(x) &= b \sum_{n=0}^{\infty} \left\{ b^{n/2} \left( \frac{1}{3} \mathcal{K}_{3,n}(x) - \frac{1}{3} \mathcal{K}_{7,n}(x) \right) \right\}, \\ \mathcal{K}_2(x) &= \sum_{n=0}^{\infty} \left\{ b^{n/2} \left( \frac{1}{2} \mathcal{K}_{3,n}(x) + \frac{1}{2} \mathcal{K}_{7,n}(x) \right) \right\}, \\ k^2 \equiv q(\omega) &= \sum_{n=0}^{\infty} \left\{ b^{n/2} q_n(\omega) \right\}, \end{aligned} \quad (2.49)$$

we find from (2.27)-(2.29) that at each order  $n \geq 1$  the equations of motion for  $\{F_n, \mathcal{K}_{3,n-1}, \mathcal{K}_{7,n-1}\}$  decouple:

$$0 = F_n'' - \frac{F_n'}{1-x} + \frac{1}{16(2x-x^2)^{3/2}} \left( \frac{\omega^2}{(1-x)^2} - q_0 \right) F_n + \frac{3F_n}{4(2x-x^2)^2} + \mathcal{J}_F^{[n]}, \quad (2.50)$$

$$0 = \mathcal{K}_{3,n}'' - \frac{\mathcal{K}_{3,n}'}{1-x} + \frac{1}{16(2x-x^2)^{3/2}} \left( \frac{\omega^2}{(1-x)^2} - q_0 \right) \mathcal{K}_{3,n} + \frac{3\mathcal{K}_{3,n}}{4(2x-x^2)^2} + \mathcal{J}_3^{[n]} \quad (2.51)$$

$$0 = \mathcal{K}_{7,n}'' - \frac{\mathcal{K}_{7,n}'}{1-x} + \frac{1}{16(2x-x^2)^{3/2}} \left( \frac{\omega^2}{(1-x)^2} - q_0 \right) \mathcal{K}_{7,n} - \frac{21\mathcal{K}_{7,n}}{4(2x-x^2)^2} + \mathcal{J}_7^{[n]}, \quad (2.52)$$

where the source terms  $\{\mathcal{J}_F^{[n]}, \mathcal{J}_3^{[n]}, \mathcal{J}_7^{[n]}\}$  are functionals of the lower order solutions,  $\{F_m, \mathcal{K}_{3,m}, \mathcal{K}_{7,m}; \xi_{2m}, \eta_{2m}, \kappa_{2m}, \zeta_{2m}\}$  and  $q_m$ , with  $m < n$ ; additionally  $\{\mathcal{J}_3^{[n]}, \mathcal{J}_7^{[n]}\}$  also depend on  $F_n$ .

The source functionals  $\mathcal{J}_F^{[1]}$ ,  $\mathcal{J}_3^{[0]}$  and  $\mathcal{J}_7^{[0]}$  identically vanish. Consider a free, minimally coupled gravitational bulk scalar  $\phi$  in  $AdS_5$ , dual to an operator of dimension  $\Delta$  of the boundary conformal theory. In  $AdS_5$ -Schwarzschild black hole background (2.41) the corresponding QNM equation takes form<sup>12</sup>

$$0 = \phi'' - \frac{\phi'}{1-x} + \frac{1}{16(2x-x^2)^{3/2}} \left( \frac{\omega^2}{(1-x)^2} - k^2 \right) \phi - \frac{\Delta(\Delta-4)\phi}{4(2x-x^2)^2}. \quad (2.53)$$

---

<sup>12</sup>Solving this equation with  $k = 0$  we reproduce the QNM spectra of  $AdS_5$ -Schwarzschild reported in [18].

Thus, we identify  $F_1$  and  $\mathcal{K}_{3,0}$  with the gravitational duals to a pair of the dimension  $\Delta = 3$  operators, and  $\mathcal{K}_{7,0}$  with the gravitational dual to the dimension  $\Delta = 7$  operator.

We can now identify distinct branches of the quasinormal modes of the KT black hole:

- The  $\mathcal{B}_7$  branch is defined by the boundary conditions

$$\mathcal{K}_{3,0}(x) \equiv 0, \quad \mathcal{K}_{7,0}(x) = x^{7/4} (1 + \mathcal{O}(x^{1/2})) , \quad (2.54)$$

where we fixed to unity the normalizable coefficient of  $\mathcal{K}_{7,0}$ . This branch is analytic in the conformal deformation parameter  $b$ : for all  $k \geq 0$ ,  $F_{2k+1}$ ,  $\mathcal{K}_{3,2k+1}$  and  $\mathcal{K}_{7,2k+1}$  vanish identically. We construct the  $\mathcal{B}_7$  branch to order  $\mathcal{O}(b)$  in appendix A.

- A pair of  $\Delta = 3$  QNM branches is defined by the boundary conditions

$$\mathcal{K}_{3,0}(x) = x^{3/4} (1 + \mathcal{O}(x^{1/2})) , \quad \mathcal{K}_{7,0}(x) \equiv 0, \quad F_1 = \alpha_0 \mathcal{K}_{3,0}, \quad (2.55)$$

where  $\alpha_0 \neq 0$  is a constant, which is fixed at the subleading order. As in (2.54), we fixed to unity the normalizable coefficient of  $\mathcal{K}_{3,0}$ . As we explain in appendix B, there are two possible choices of  $\alpha_0$ , differing by the overall sign — this leads to two possible values of  $q_1$ ,

$$q = q_0 \pm |q_1| b^{1/2} + \mathcal{O}(b). \quad (2.56)$$

We call the ‘+’ branch in (2.56)  $\mathcal{B}_{3u}$  — as we follow this branch to low temperatures, it identifies QNMs spontaneously breaking the chiral symmetry<sup>13</sup>. The other branch, the ‘-’ branch in (2.56) — we call it  $\mathcal{B}_{3s}$  — represents the stable quasinormal modes.

### 3 KS branches from explicit $\chi$ SB fluctuations of the KT black hole

There is an alternative approach to identify spontaneous symmetry broken phases in holographic duals advocated in [21]. Unlike the analysis of the QNMs in the symmetry breaking sector, it does not identify exactly what mode becomes unstable, but it does determine the onset of the instability. The idea is simple. The homogeneous and isotropic “branches” of the symmetry-broken KS black hole connect to the KT black hole “trunk” wherever the parameters of the latter allow for a linearized normalizable fluctuations in the symmetry breaking sector. If, exactly at the onset of the instability,

---

<sup>13</sup>This is the branch of the QNMs originally found in [2].

one turns on a non-normalizable coefficient for the fluctuations, their normalizable coefficients will necessarily diverge. Thus, a way to identify onset of the  $\chi$ SB instabilities of the KT black hole is to monitor for the divergence of the expectation values of the condensates (such as parameters  $\{f_{3,0}, k_{2,3,0}, k_{2,7,0}\}$  in (2.33)-(2.35) ) as the KT hole temperature varies, provided we turn on the non-normalizable coefficient — here, a gravitational dual to one of the gaugino mass parameters [2].

The relevant set of equations is (2.27)-(2.29) with  $\omega = k = 0$ . We use the computational SchemeA (see section 2.3), *i.e.*, we set  $P = a_0 = g_0 = 1$  and vary  $k_s$  parameter of the KT black hole. It is possible to turn on two independent non-normalizable coefficients  $\mu_1$  and  $\mu_2$  in the chiral symmetry breaking sector:

$$\begin{aligned} F = & \left( \mu_1(k_s + 2) - \left( \frac{1}{2}\mu_1 + \mu_2 \right) \ln x \right) x^{1/4} + f_{3,0}x^{3/4} + \left( \frac{249}{2}f_{3,2,0}\mu_1 + 83\mu_2f_{3,2,0} \right. \\ & - \frac{1}{4}g_{2,0}\mu_1 - \frac{1}{2}\mu_2g_{2,0} + \frac{1}{8}\mu_1k_s + \frac{77}{2}f_{3,2,0}\mu_1k_s - 6\mu_2f_{3,2,0}k_s - \frac{1}{2}\mu_2 + \left( -\frac{71}{4}f_{3,2,0}\mu_1 \right. \\ & - \frac{71}{2}\mu_2f_{3,2,0} - \frac{1}{16}\mu_1 - \frac{1}{8}\mu_2 \left. \right) \ln x \left. \right) x^{5/4} + \left( f_{7,0} + \left( -6f_{3,0}f_{3,2,0} - \frac{3}{2}f_{3,3,0}\mu_1 \right. \right. \\ & \left. \left. - 3f_{3,3,0}\mu_2 \right) \ln x \right) x^{7/4} + \mathcal{O}(x^{9/4} \ln^3 x), \end{aligned} \quad (3.1)$$

$$\mathcal{K}_1 = \mu_2(k_s + 2)x^{1/4} + \left( k_{1,3,0} + \frac{1}{2}f_{3,0} \ln x \right) x^{3/4} + \mathcal{O}(x^{5/4} \ln^2 x), \quad (3.2)$$

$$\begin{aligned} \mathcal{K}_2 = & \left( -\frac{3}{2}\mu_1k_s + \frac{3}{2}k_s\mu_2 - \frac{15}{4}\mu_1 + \frac{3}{2}\mu_2 + \left( \frac{3}{4}\mu_1 + \frac{3}{2}\mu_2 \right) \ln x \right) x^{1/4} + \left( -f_{3,0} + \frac{3}{2}k_{1,3,0} \right. \\ & \left. + \frac{3}{4}f_{3,0} \ln x \right) x^{3/4} + \mathcal{O}(x^{5/4} \ln^2 x), \end{aligned} \quad (3.3)$$

where the normalizable near the boundary, *i.e.*, as  $x \rightarrow 0_+$ , coefficients are

$$\{f_{3,0}, k_{1,3,0}, f_{7,0}\}. \quad (3.4)$$

In the IR we have the asymptotic expansion as in (2.38).

Precisely how we turn on the non-normalizable parameters is irrelevant — what matters is that  $\mu_i$ 's are not simultaneously zero. We set  $\mu_1 = 0$  and  $\mu_2 = 1$ . The numerical results for the normalizable coefficients (3.4) are presented in fig. 5. All the normalizable coefficients diverge at  $T = T_{\chi\text{SB}} \equiv 0.54195\Lambda$ , denoted by the vertical

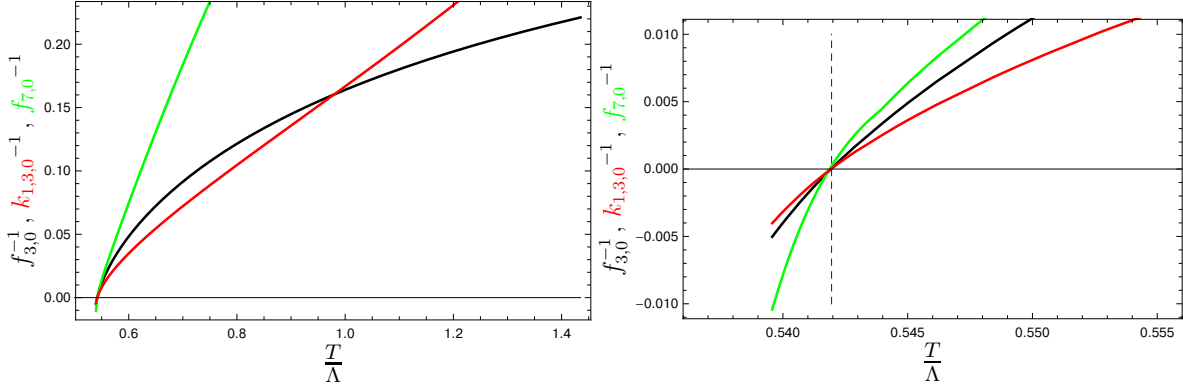


Figure 5: Inverses of the normalizable coefficients  $f_{3,0}$ ,  $k_{1,3,0}$ ,  $f_{7,0}$  (see (3.1)-(3.3)) of the static homogeneous linearized chiral symmetry breaking fluctuations about the KT black hole background as functions of the KT black hole temperature. The nonnormalizable coefficients are set as  $\mu_1 = 0$  and  $\mu_2 = 1$ . All the normalizable coefficients diverge at  $T = T_{\chi\text{SB}}$  (a vertical dashed blue line in the right panel); there are no additional divergences for  $T > T_{\chi\text{SB}}$ .

dashed blue line (see the right panel) — this is the  $\chi\text{SB}$  instability identified in [2]. There are no other divergences for  $T > T_{\chi\text{SB}}$ . Once again, we conclude that there are no additional KS black hole branches beyond the one identified in [2] and constructed in [1].

## Acknowledgments

Research at Perimeter Institute is supported by the Government of Canada through Industry Canada and by the Province of Ontario through the Ministry of Research & Innovation. This work was further supported by NSERC through the Discovery Grants program.

## A $\mathcal{B}_7$ branch of the QNMs of the KT black hole in the $b \rightarrow 0$ conformal limit

We construct here  $\mathcal{B}_7$  branch to order  $\mathcal{O}(b)$ . The relevant equations of motion at  $\omega = 0$  are

$$0 = \mathcal{K}_{7,0}'' - \frac{\mathcal{K}_{7,0}'}{1-x} - \frac{q_0 \mathcal{K}_{7,0}}{16(2x-x^2)^{3/2}} - \frac{21\mathcal{K}_{7,0}}{4(2x-x^2)^2}, \quad (\text{A.1})$$

at order  $\mathcal{O}(b^0)$ , and

$$\begin{aligned} 0 = & F_2'' - \frac{F_2'}{1-x} - \frac{q_0 F_2}{16(2x-x^2)^{3/2}} + \frac{3F_2}{4(2x-x^2)^2 x^2} + \frac{2}{3} \kappa_2' \mathcal{K}_{7,0}' - \frac{\mathcal{K}_{7,0}}{(2x-x^2)^2}, \quad (\text{A.2}) \\ 0 = & \mathcal{K}_{7,2}'' - \frac{\mathcal{K}_{7,2}'}{1-x} - \frac{q_0 \mathcal{K}_{7,2}}{16(2x-x^2)^{3/2}} - \frac{21\mathcal{K}_{7,2}}{4(2x-x^2)^2} - \frac{\mathcal{K}_{7,0} q_2}{16(2x-x^2)^{3/2}} - 3\kappa_2' F_2' \\ & - \frac{21F_2}{2(2x-x^2)^2} + \left(3\eta_2' + \frac{2}{5}\lambda_2'\right) \mathcal{K}_{7,0}' + \left(\left(\frac{q_0}{48}\sqrt{2x-x^2} + \frac{7}{4}\right) (\kappa_2')^2 - \frac{(x^2-2x+2)}{(2x-x^2)(1-x)}\right. \\ & \times \left(\frac{q_0}{8}\sqrt{2x-x^2} + \frac{21}{2}\right) \xi_2' - \frac{1}{48(2x-x^2)^2} (480\kappa_2 + 1440\eta_2 - 144\lambda_2 + 84 + q_0\sqrt{2x-x^2}) \\ & \left. \times (4\kappa_2 + 6\xi_2 + 1)\right) \mathcal{K}_{7,0}, \quad (\text{A.3}) \end{aligned}$$

$$\begin{aligned} 0 = & \mathcal{K}_{3,2}'' - \frac{\mathcal{K}_{3,2}'}{1-x} - \frac{q_0 \mathcal{K}_{3,2}}{16(2x-x^2)^{3/2}} + \frac{3\mathcal{K}_{3,2}}{4(2x-x^2)^2} + \zeta_2' \mathcal{K}_{7,0}' + 3\kappa_2' F_2' + \frac{3F_2}{2(2x-x^2)^2} \\ & + \frac{3\zeta_2 \mathcal{K}_{7,0}}{(2x-x^2)^2}, \quad (\text{A.4}) \end{aligned}$$

at order  $\mathcal{O}(b^1)$ . Additionally,  $F_1(x) = \mathcal{K}_{3,0}(x) = \mathcal{K}_{3,1}(x) = \mathcal{K}_{7,1}(x) \equiv 0$  and  $q_1 = 0$ .

The asymptotic expansions near the boundary, *i.e.*, as  $x \rightarrow 0_+$ ,

$$\mathcal{K}_{7,0} = x^{7/4} \left(1 + \frac{\sqrt{2}}{96} q_0 x^{1/2} + \mathcal{O}(x)\right), \quad (\text{A.5})$$

$$F_2 = x^{3/4} \left(f_{2,3,0} + \frac{\sqrt{2}}{32} q_0 f_{2,3,0} x^{1/2} + \mathcal{O}(x)\right), \quad (\text{A.6})$$

$$\begin{aligned}
\mathcal{K}_{7,2} = & x^{3/4} \left( -f_{2;3,0} - \frac{\sqrt{2}}{128} q_0 f_{2;3,0} x^{1/2} + \left( k_{7,2;7,0} - \left( \frac{1}{2} - \frac{9f_{2;3,0}}{20} + \frac{q_0^2 f_{2;3,0}}{10240} \right) \ln x \right) x \right. \\
& + x^{3/2} \left( \frac{\sqrt{2}}{96} q_2 - \left( \frac{q_0^3 \sqrt{2}}{983040} f_{2;3,0} - \frac{3\sqrt{2}}{640} q_0 f_{2;3,0} + \frac{\sqrt{2}}{96} q_0 \right) \ln x + \frac{\sqrt{2}}{1474560} q_0^3 f_{2;3,0} \right. \\
& \left. \left. + \frac{517\sqrt{2}}{15360} q_0 f_{2;3,0} + \frac{\sqrt{2}}{96} k_{7,2;7,0} q_0 + \frac{55\sqrt{2}}{3456} q_0 \right) + \mathcal{O}(x^2 \ln x) \right), \tag{A.7}
\end{aligned}$$

$$\begin{aligned}
\mathcal{K}_{3,2} = & x^{3/4} \left( \frac{3}{2} f_{2;3,0} \ln x + k_{3,2;3,0} + x^{1/2} \left( \frac{3\sqrt{2}}{64} f_{2;3,0} \ln x - \frac{3\sqrt{2}}{64} f_{2;3,0} + \frac{\sqrt{2}}{32} k_{3,2;3,0} \right) q_0 \right. \\
& \left. + \mathcal{O}(x \ln x) \right), \tag{A.8}
\end{aligned}$$

are characterized by

$$\{q_0, f_{2;3,0}, q_2, k_{7,2;7,0}, k_{3,2;3,0}\}. \tag{A.9}$$

As part of the overall normalization, we can set

$$k_{7,2;7,0} = 0. \tag{A.10}$$

Near the black hole horizon, *i.e.*, as  $y \equiv 1 - x \rightarrow 0_+$ ,

$$\begin{aligned}
\mathcal{K}_{7,0} &= k_{7,0;0}^h + \mathcal{O}(y^2), & F_2 &= f_{2;0}^h + \mathcal{O}(y^2), \\
\mathcal{K}_{7,2} &= k_{7,2;0}^h + \mathcal{O}(y^2), & \mathcal{K}_{3,2} &= k_{3,2;0}^h + \mathcal{O}(y^2),
\end{aligned} \tag{A.11}$$

characterized by

$$\{k_{7,0;0}^h, f_{2;0}^h, k_{7,2;0}^h, k_{3,2;0}^h\}. \tag{A.12}$$

In total we have  $5 + 4 - 1 = 8$  (from (A.9) and (A.11) minus the constraint (A.10)) parameters to numerically solve the system of four second-order ODEs (A.1)-(A.4). Discrete solutions are characterized by the number of nodes in the radial wavefunction  $\mathcal{K}_{7,0}$  — this is the tower of the excited QNMs on the  $\mathcal{B}_7$  branch. We focus on the lowest QNM on the branch, *i.e.*, we require that  $\mathcal{K}_{7,0}$  does not have nodes. For the lowest QNM on the  $\mathcal{B}_7$  branch we find:

$q_0$	$f_{2;3,0}$	$q_2$	$k_{3,2;3,0}$	$k_{7,0;0}^h$	$f_{2;0}^h$	$k_{7,2;0}^h$	$k_{3,2;0}^h$
-164.395	0.153	185.391	0.383	0.0828	0.0297	-0.200	-0.0720

Note that

$$q^2 \equiv \frac{q}{(2\pi T)^2} = \frac{q_0}{16} + \frac{1}{32} \left( (1 + \ln 2) q_0 + 2 q_2 \right) b + \mathcal{O}(b^2), \quad (\text{A.13})$$

where we used (2.47). The high-temperature approximation (A.13) to the QNM branch  $\mathcal{B}_7$  is shown as a dashed green line on the right panel of fig. 2.

## B $\mathcal{B}_{3u}$ and $\mathcal{B}_{3s}$ branches of the KT black hole QNMs in the $\sqrt{b} \rightarrow 0$ conformal limit

We construct here  $\mathcal{B}_{3u}$  and  $\mathcal{B}_{3s}$  branches to order  $\mathcal{O}(\sqrt{b})$ . The relevant equations of motion at  $\omega = 0$  are

$$0 = \mathcal{K}_{3,0}'' - \frac{\mathcal{K}_{3,0}'}{1-x} - \frac{q_0 \mathcal{K}_{3,0}}{16(2x-x^2)^{3/2}} = \frac{3\mathcal{K}_{3,0}}{4(2x-x^2)^2}, \quad (\text{B.1})$$

at order  $\mathcal{O}(b^0)$ , and

$$0 = F_2'' - \frac{F_2'}{1-x} - \frac{q_0 F_2}{16(2x-x^2)^{3/2}} + \frac{3F_2}{4(2x-x^2)^2 x^2} - \frac{2}{3} \kappa_2' \mathcal{K}_{3,0}' - \frac{\mathcal{K}_{3,0}}{(2x-x^2)^2} - \frac{\alpha_0 q_1 \mathcal{K}_{3,0}}{16(2x-x^2)^{3/2}}, \quad (\text{B.2})$$

$$0 = \mathcal{K}_{3,1}'' - \frac{\mathcal{K}_{3,1}'}{1-x} - \frac{q_0 \mathcal{K}_{3,1}}{16(2x-x^2)^{3/2}} + \frac{3\mathcal{K}_{3,1}}{4(2x-x^2)^2} + 3\alpha_0 \kappa_2' \mathcal{K}_{3,0}' + \frac{3\alpha_0 \mathcal{K}_{3,0}}{2(2x-x^2)^2} - \frac{q_1 \mathcal{K}_{3,0}}{16(2x-x^2)^{3/2}}, \quad (\text{B.3})$$

$$0 = \mathcal{K}_{7,1}'' - \frac{\mathcal{K}_{7,1}'}{1-x} - \frac{q_0 \mathcal{K}_{7,1}}{16(2x-x^2)^{3/2}} - \frac{21\mathcal{K}_{7,1}}{4(2x-x^2)^2} - 3\alpha_0 \kappa_2' \mathcal{K}_{3,0}' - \frac{21\alpha_0 \mathcal{K}_{3,0}}{2(2x-x^2)^2}, \quad (\text{B.4})$$

at order  $\mathcal{O}(\sqrt{b})$ . Additionally,  $F_1(x) \equiv \alpha_0 \mathcal{K}_{3,0}(x)$ ,  $\mathcal{K}_{7,0}(x) \equiv 0$ . Note that (B.2)-(B.4) have a  $\mathbb{Z}_2$  symmetry:

$$\{F_2(x), \mathcal{K}_{3,1}(x), \mathcal{K}_{7,1}(x), \alpha_0, q_1\} \iff \{F_2(x), -\mathcal{K}_{3,1}(x), -\mathcal{K}_{7,1}(x), -\alpha_0, -q_1\}. \quad (\text{B.5})$$

Both equations (B.2) and (B.3) have zero modes: if  $\{F_2, \mathcal{K}_{3,1}\}$  are solutions, for arbitrary constants  $\alpha_1$  and  $\beta$ ,

$$F_2 \rightarrow F_2 + \alpha_1 \mathcal{K}_{3,0}, \quad \mathcal{K}_{3,1} \rightarrow \mathcal{K}_{3,1} + \beta \mathcal{K}_{3,0}, \quad (\text{B.6})$$

are solutions as well. The constant  $\beta$  is absorbed into the overall normalization of the linearized fluctuations; and the constant  $\alpha_1$  is fixed at order  $\mathcal{O}(b)$ , similar to how the constant  $\alpha_0$  is fixed at order  $\mathcal{O}(\sqrt{b})$ , as discussed below.

The asymptotic expansions near the boundary, *i.e.*, as  $x \rightarrow 0_+$ ,

$$\mathcal{K}_{3,0} = x^{3/4} \left( 1 + \frac{\sqrt{2}}{32} q_0 x^{1/2} + \mathcal{O}(x) \right), \quad (\text{B.7})$$

$$F_2 = x^{3/4} \left( f_{2;3,0} + \frac{\sqrt{2}}{96} \left( 3\alpha_0 q_1 + q_0(3f_{2;3,0} - 1) \right) x^{1/2} + \mathcal{O}(x) \right), \quad (\text{B.8})$$

$$\begin{aligned} \mathcal{K}_{3,1} = x^{3/4} & \left( \frac{3}{2} \alpha_0 \ln x + k_{3,1;3,0} + x^{1/2} \left( \frac{3\sqrt{2}\alpha_0 q_0}{64} \ln x - \frac{\sqrt{2}}{64} (3\alpha_0 q_0 - 2k_{3,1,3,0} q_0 - 2q_1) \right) \right. \\ & \left. + \mathcal{O}(x \ln x) \right), \end{aligned} \quad (\text{B.9})$$

$$\begin{aligned} \mathcal{K}_{7,1} = x^{3/4} & \left( -\alpha_0 - \frac{\sqrt{2}\alpha_0 q_0}{128} x^{1/2} + \left( k_{7,1;7,0} + \left( \frac{9\alpha_0}{20} - \frac{\alpha_0 q_0^2}{10240} \right) \ln x \right) x \right. \\ & \left. + \mathcal{O}(x^{3/2} \ln x) \right), \end{aligned} \quad (\text{B.10})$$

are characterized by

$$\{q_0, f_{2;3,0}, \alpha_0, q_1, k_{3,1;3,0}, k_{7,1;7,0}\}. \quad (\text{B.11})$$

As part of the overall normalization (choosing  $\beta$  in (B.6)), we can set

$$k_{3,1;3,0} = 0. \quad (\text{B.12})$$

Furthermore,  $f_{2;3,0} = \alpha_1$  as defined in (B.6) — it remains free at this order, but is fixed at  $\mathcal{O}(b)$  order. Near the black hole horizon, *i.e.*, as  $y \equiv 1 - x \rightarrow 0_+$ ,

$$\begin{aligned} \mathcal{K}_{3,0} &= k_{3,0;0}^h + \mathcal{O}(y^2), & F_2 &= f_{2,0}^h + \mathcal{O}(y^2), \\ \mathcal{K}_{3,1} &= k_{3,1;0}^h + \mathcal{O}(y^2), & \mathcal{K}_{7,1} &= k_{7,1;0}^h + \mathcal{O}(y^2), \end{aligned} \quad (\text{B.13})$$

characterized by

$$\{k_{3,0;0}^h, f_{2,0}^h, k_{3,1;0}^h, k_{7,1;0}^h\}. \quad (\text{B.14})$$

In total we have  $6 + 4 - 1 - 1 = 8$  (from (B.11) and (B.14) minus the constraint (B.12) and minus the free value of  $\alpha_1$ ) parameters to numerically solve the system of four



second-order ODEs (B.1)-(B.4). The symmetry (B.5) implies the symmetry in  $\mathcal{O}(\sqrt{b})$  parameters:

$$\{\alpha_0, q_1, k_{7,1;7,0}^h, f_{2,0}^h, k_{3,1;0}^h, k_{7,1;0}^h\} \iff \{-\alpha_0, -q_1, -k_{7,1;7,0}^h, f_{2,0}^h, -k_{3,1;0}^h, -k_{7,1;0}^h\}. \quad (\text{B.15})$$

Discrete solutions are characterized by the number of nodes in the radial wavefunction  $\mathcal{K}_{3,0}$  — this is the tower of the excited QNMs. Additionally,  $\mathbb{Z}_2$  symmetry (B.5) implies that at order  $\mathcal{O}(\sqrt{b})$  there are actually 2 separate branches,  $\mathcal{B}_{3u}$  and  $\mathcal{B}_{3s}$ , coalescing at  $b = 0$ . This  $\mathbb{Z}_2$  symmetry exchanges the branches, see (2.56). We focus on the lowest QNMs on each branch, *i.e.*, we require that  $\mathcal{K}_{3,0}$  does not have nodes. For these lowest QNMs on  $\mathcal{B}_{3u}/\mathcal{B}_{3s}$  (correspondingly  $+/-$  signs in the table for  $q_1$ ) branches we find:

$q_0$	$\alpha_0$	$q_1$	$k_{7,1;7,0}^h$	$k_{3,0;0}^h$	$f_{2,0}^h$	$k_{3,1;0}^h$	$k_{7,1;0}^h$
-22.969	$\mp 0.471$	$\pm 27.434$	$\mp 0.522$	0.350	-0.0432	$\pm 0.263$	$\pm 0.261$

Note that

$$\mathfrak{q}^2 \equiv \frac{q}{(2\pi T)^2} = \frac{1}{16} \left( q_0 \pm |q_1| \sqrt{b} \right) + \mathcal{O}(b). \quad (\text{B.16})$$

The high-temperature approximations (B.16) to the QNM branches  $\mathcal{B}_{3u}/\mathcal{B}_{3s}$  are shown as dashed black/red lines on the right panel of fig. 1.

## References

- [1] A. Buchel, *Klebanov-Strassler black hole*, *JHEP* **01** (2019) 207, [1809.08484].
- [2] A. Buchel, *Chiral symmetry breaking in cascading gauge theory plasma*, *Nucl. Phys.* **B847** (2011) 297–324, [1012.2404].
- [3] O. Aharony, A. Buchel and P. Kerner, *The Black hole in the throat: Thermodynamics of strongly coupled cascading gauge theories*, *Phys. Rev.* **D76** (2007) 086005, [0706.1768].
- [4] C. P. Herzog, I. R. Klebanov and P. Ouyang, *Remarks on the warped deformed conifold*, in *Modern Trends in String Theory: 2nd Lisbon School on g Theory Superstrings Lisbon, Portugal, July 13-17, 2001*, 2001. **hep-th/0108101**.

- [5] I. R. Klebanov and M. J. Strassler, *Supergravity and a confining gauge theory: Duality cascades and chi SB resolution of naked singularities*, *JHEP* **08** (2000) 052, [[hep-th/0007191](#)].
- [6] A. Buchel, *Finite temperature resolution of the Klebanov-Tseytlin singularity*, *Nucl. Phys.* **B600** (2001) 219–234, [[hep-th/0011146](#)].
- [7] A. Buchel, C. P. Herzog, I. R. Klebanov, L. A. Pando Zayas and A. A. Tseytlin, *Nonextremal gravity duals for fractional D-3 branes on the conifold*, *JHEP* **04** (2001) 033, [[hep-th/0102105](#)].
- [8] S. S. Gubser, C. P. Herzog, I. R. Klebanov and A. A. Tseytlin, *Restoration of chiral symmetry: A Supergravity perspective*, *JHEP* **05** (2001) 028, [[hep-th/0102172](#)].
- [9] O. Aharony, A. Buchel and A. Yarom, *Holographic renormalization of cascading gauge theories*, *Phys. Rev.* **D72** (2005) 066003, [[hep-th/0506002](#)].
- [10] I. Bena, A. Buchel and S. Lust, *Throat destabilization (for profit and for fun)*, [1910.08094](#).
- [11] A. Buchel, *A Holographic perspective on Gubser-Mitra conjecture*, *Nucl. Phys.* **B731** (2005) 109–124, [[hep-th/0507275](#)].
- [12] A. Buchel and C. Pagnutti, *Exotic Hairy Black Holes*, *Nucl. Phys. B* **824** (2010) 85–94, [[0904.1716](#)].
- [13] A. Buchel, *Hydrodynamics of the cascading plasma*, *Nucl. Phys. B* **820** (2009) 385–416, [[0903.3605](#)].
- [14] D. Nickel, *Inhomogeneous phases in the Nambu-Jona-Lasino and quark-meson model*, *Phys. Rev. D* **80** (2009) 074025, [[0906.5295](#)].
- [15] A. Donos and J. P. Gauntlett, *Holographic striped phases*, *JHEP* **08** (2011) 140, [[1106.2004](#)].
- [16] F. Gross and J. Milana, *Decoupling confinement and chiral symmetry breaking: An Explicit model*, *Phys. Rev. D* **45** (1992) 969–974.

- [17] O. Aharony, J. Sonnenschein and S. Yankielowicz, *A Holographic model of deconfinement and chiral symmetry restoration*, *Annals Phys.* **322** (2007) 1420–1443, [[hep-th/0604161](#)].
- [18] A. Nunez and A. O. Starinets, *AdS / CFT correspondence, quasinormal modes, and thermal correlators in  $N=4$  SYM*, *Phys. Rev. D* **67** (2003) 124013, [[hep-th/0302026](#)].
- [19] A. Buchel, *Quantum phase transitions in cascading gauge theory*, *Nucl. Phys. B* **856** (2012) 278–327, [[1108.6070](#)].
- [20] P. K. Kovtun and A. O. Starinets, *Quasinormal modes and holography*, *Phys. Rev. D* **72** (2005) 086009, [[hep-th/0506184](#)].
- [21] A. Buchel,  *$\chi$ SB of cascading gauge theory in de Sitter*, [1912.03566](#).